A dual-polarization QPE method based on the NCAR Particle ID algorithm Description and preliminary results

Michael J. Dixon[1], J. W. Wilson[1], T. M. Weckwerth[1], D. Albo[1] and E. J. Thompson[2]

1: National Center for Atmospheric Research (NCAR), Boulder, Colorado
2: Colorado State University, Fort Collins, Colorado
NCAR is sponsored by the National Science Foundation

9A.1
AMS 37th Conference on Radar Meteorology
Norman, Oklahoma, USA
2015-09-17

1 Introduction

Radar-based Quantitative Precipitation Estimation (QPE) for precipitation at the surface requires three fundamental steps: (a) estimation of the precipitation rate aloft within the radar volume; (b) estimation of the applicable rate at the surface; and (c) conversion from rate to precipitation depth over some period of time.

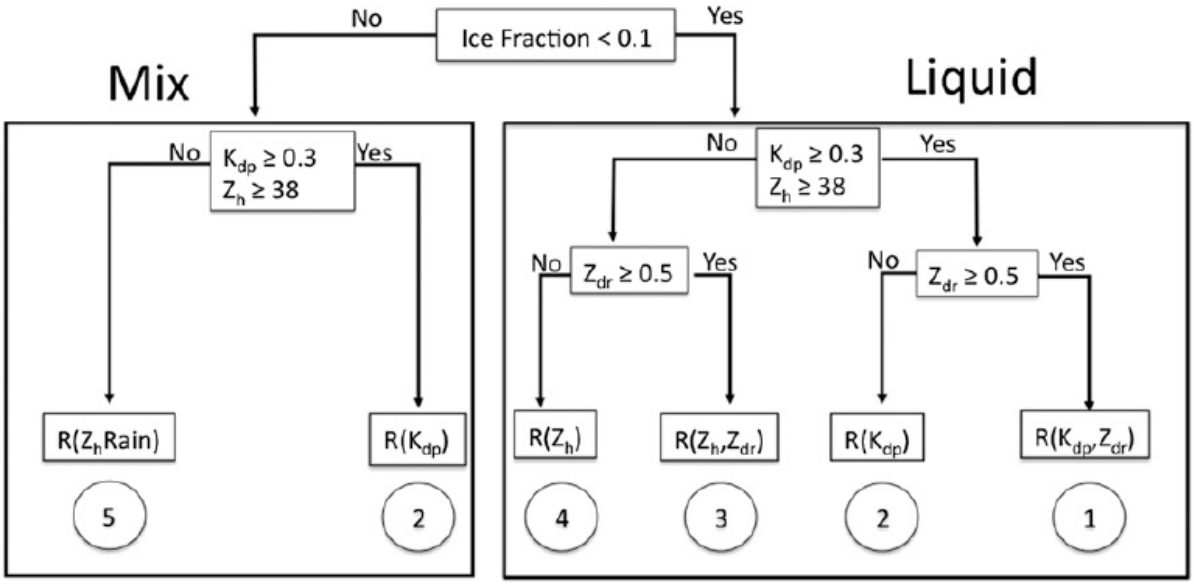

Figure 1: Flowchart describing the CSU-ICE algorithm (Cifelli et al., 2011).

A significant number of algorithms have been employed for the estimation of precipitation rate from dual-polarization radar data. Estimators have been proposed based on a variety of combinations of dual-polarization variables (Sachidananda and Zrnic1987; Brandes et al. 2002). These individual estimators have also been combined into so-called 'hybrid' estimators by selecting the estimator most appropriate to a particular situation, generally based on the value of

the dual-polarization variables at that location (Ryzhkov et al. 2005; Bringi et al. 2009, Pepler et al. 2011; Cifelli et al. 2011; Kim and Maki 2012). For example, Fig. 1 shows the combinatorial logic from Cifelli et al. (2011) for S-band:

Similarly, Fig. 2 shows the logic used by Bringi et al. (2009) for C-band:

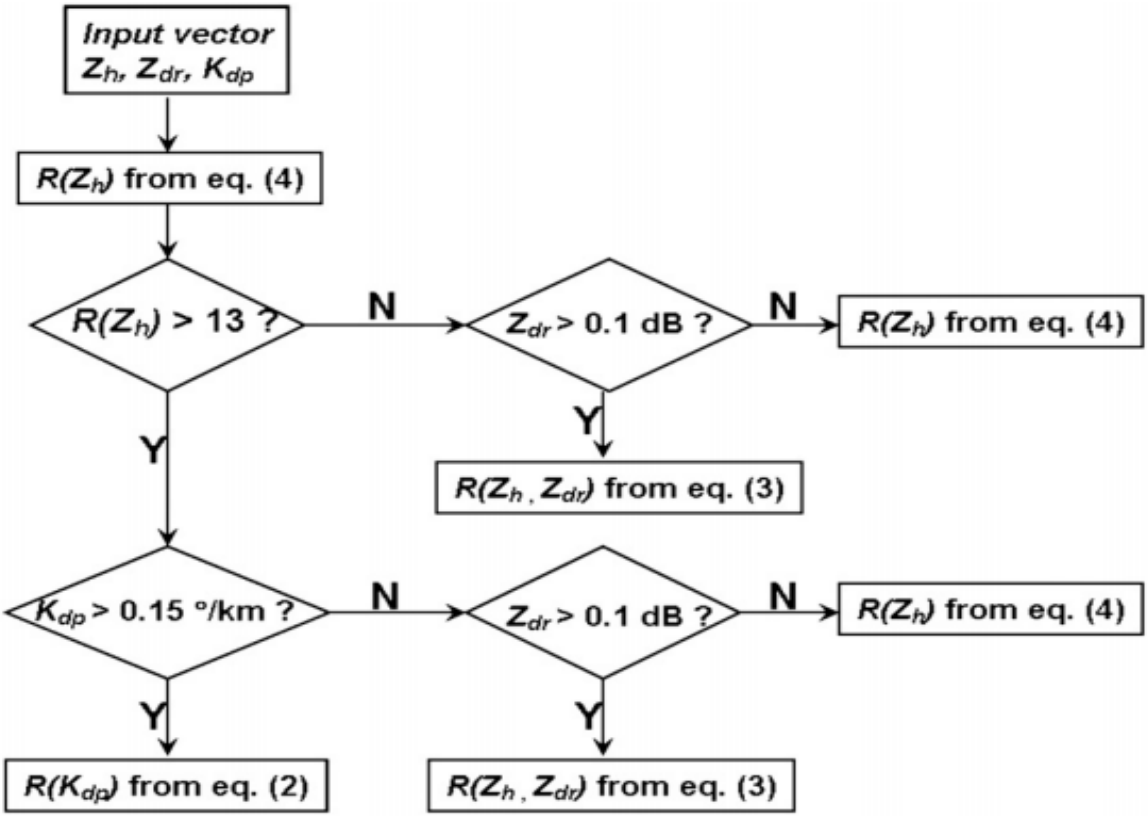

Figure 2: Block diagram illustrating the rain-rate retrieval method using a variant of the Ryzhkov et al. (2005) approach and adapted for C-band. (Bringi et al. 2009).

These hybrid methods produce results that are superior to those from individual estimators. However, as can be seen from the above figures, the methods depend on the correct choice of a considerable number of thresholds from which decisions are made in the rule-based tree. In decision systems such as these, adopting thresholds necessarily requires discarding some of the possible options, and can lead to results that are less than optimal. Furthermore, tuning the thresholds can be time consuming and error-prone.

As an alternative to the threshold-based hybrid techniques, a hydrometeor classification algorithm can be used to determine which rate relationship is appropriate (Giangrande and Ryzhkov 2008; Berkowitz et al. 2013).This approach has the advantage that determination of the thresholds is not required in the QPE step because the hydrometeor classification algorithms on which they are based make use of fuzzy logic for the determination of the hydrometeor type (Vivekanandan et al. 1999; Lim et al. 2005; Park et al. 2009).

This is the approach that is taken in this study. The NCAR particle identification (PID) algorithm (Vivekanandan et al. 1999) is used to determine the hydrometeor type, and the choice of precipitation rate relationship is then based on the PID.

The method was originally developed for the Front Range Operational Network Testbed (FRONT) 2014 season (Hubbert et al. 2014). Based on this experience the method was refined before being deployed during the Plains Elevated Convection at Night (PECAN) field project in Kansas during the summer of 2015. The method was applied to data from the NEXRAD WSR-88D network of radars used during PECAN, along with the NCAR S-band polarization (S-POL) radar.

In section 2 we describe the method in some detail. In section 3 we show some initial results from PECAN. We follow with conclusions in section 4.

2 Method

2.1 Outline

The main steps in the NCAR QPE procedure for each individual radar are:

1. Run the NCAR particle identification (PID) algorithm;
2. Estimate the precipitation rate throughout the 3D radar volume;
3. Compute the beam blockage;
4. Compute the QPE rate at the ground in polar coordinates;
5. Transform the surface QPE rate into Cartesian coordinates.

Then, to compute the QPE depth over a region:

6. Merge the Cartesian QPE rate grids from individual radars into a single grid, every 6 minutes;
7. Compute QPE depth from rate for each 6-minute merged product;
8. Sum QPE depth over time for various accumulation periods.

2.2 Running the PID algorithm

The NCAR PID algorithm (Vivekanandan 1999) requires a temperature profile from which to estimate the 0-degree temperature height. Because routine soundings only occur every 12 hours and are not located close to the radar sites, model-based soundings are used, derived from the RUC Rapid 13-km model. The RUC data arrives mapped onto pressure levels as the vertical coordinate. The data is interpolated to remap it onto height levels relative to sea level from which the vertical profile of temperature at each radar location is estimated.

During the 2014 FRONT projects some temperature profile-related errors were observed with the PID product. Since the melting layer is the most important feature, and the wet-bulb temperature is more relevant to the melting process, it was decided to use the wet-bulb temperature rather than the dry-bulb temperature for the PID temperature profile. During PECAN the wet-bulb profiles did seem to work well for PID, but further study is required to confirm that wet-bulb temperature is preferable to dry-bulb temperature for this purpose.

2.3 Estimating precipitation rate

For each radar range gate in a volume with a signal-to-noise ratio (SNR) exceeding 5 dB, a number of precipitation estimators are computed.

In all of these estimators, the following units apply:

Zh: mm^6m^{-3}

KDP: deg/km

ZDR: linear unit-less ratio

The following rate formulations are used:

R(Z) for rain:

$$R(Z) = 0.0274Z^{0.694} \quad (1)$$

which is equivalent to:

$$Z = 178R^{1.44} \quad (2)$$

R(Z) for dry snow (i.e. above the melting layer):

$$R(Z) = 0.0365Z^{0.625} \quad (3)$$

which is equivalent to Marshall Palmer:

$$Z = 200R^{1.6} \quad (4)$$

R(Z, ZDR) (from Berkowitz 2013):

$$R(Z, ZDR) = 0.0067Z^{0.927}Zdr^{-3.43} \quad (5)$$

R(KDP) (from Berkowitz 2013):

$$R(KDP) = sign(Kdp)44|Kdp|^{0.822} \quad (6)$$

In computing the above estimators, the following limits are applied to keep the results within reasonable bounds:

dBZ <= 53. If the reflectivity exceeds 53, it is capped at 53 dBZ to avoid excessive values in the presence of hail.

R < 125 mm/hr. If the rate exceeds 125 mm/hr, it is capped at 125. This was adopted as a reasonable climatological upper bound for Eastern Colorado and Kansas.

In mixed phase regions (e.g., the melting layer) the measured reflectivity is reduced by 10 dB to account for the enhanced reflectivity in the bright-band.

2.4 NCAR Hybrid method

The NCAR HYBRID method uses the PID to determine which rate relationship to apply.

The logic diagram for the NCAR HYBRID method is shown in figure 3 below:

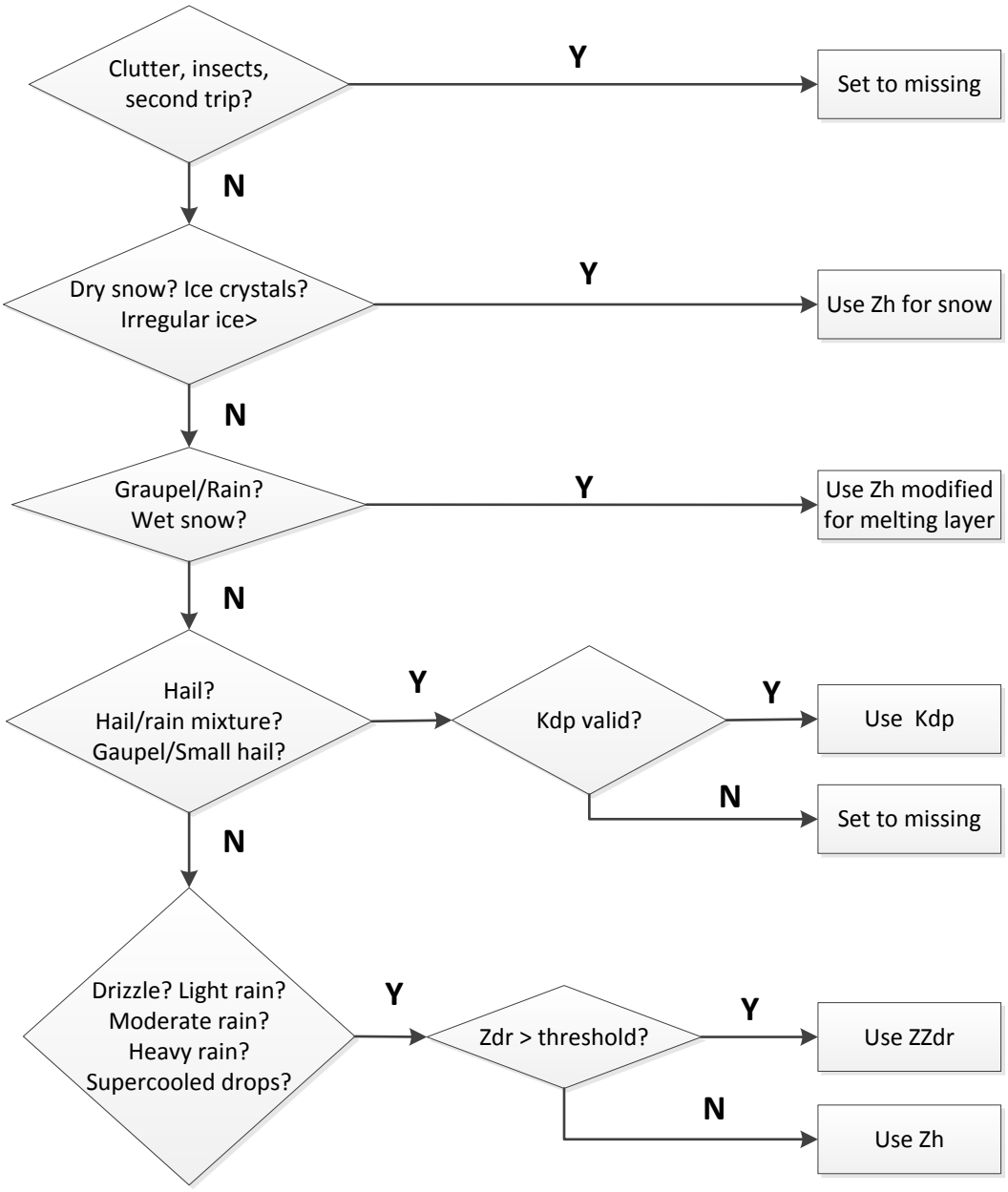

Figure 3: Logical decision tree for NCAR HYBRID algorithm.

For the HYBRID algorithm, the ZDR threshold is set to 0.5 dB.

2.5 NCAR Weighted-PID method

In the NCAR Weighted-PID method a weight is assigned to each rate relationship for each radar gate. The weights are determined from the interest values assigned to each of the of the various particle types identified by the PID algorithm. QPE is then computed as the weighted sum of the various estimators. See Fig. 4 below for the flow of logic.

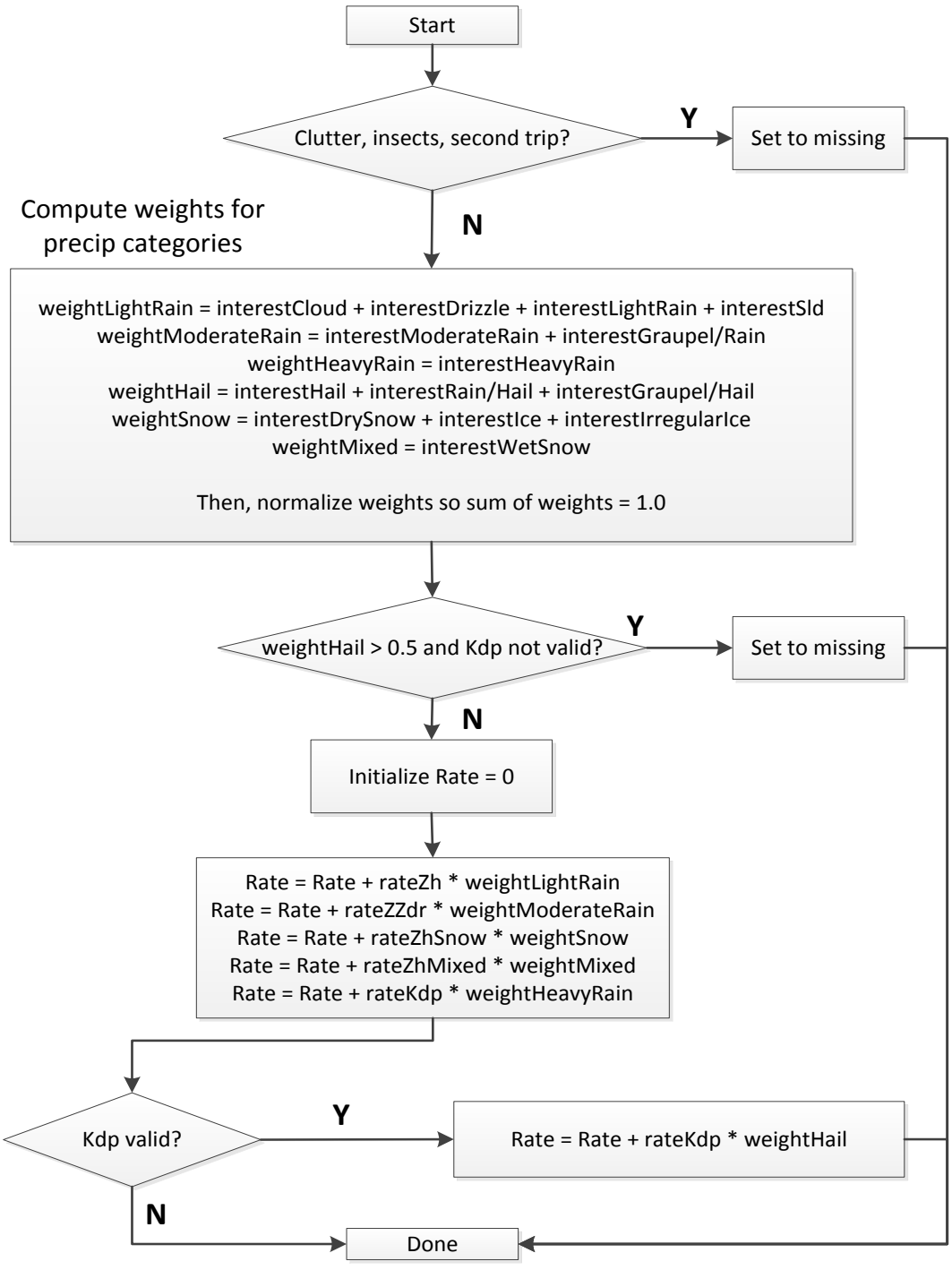

Figure 4: Logical decision tree for the NCAR Weighted-PID algorithm.

2.6 Beam blockage computations per radar

For each radar, a beam blockage algorithm is run to compute the blockage at the lower elevation angles. The algorithm makes use of the SRTM 30-m resolution digital elevation data obtained from the NASA space shuttle STS-99 mission. This data comes in 1-deg x 1-deg tiles: (http://www2.jpl.nasa.gov/srtm/cbanddataproducts.html).

The method is reasonably sophisticated and takes account of standard atmospheric propagation effects and the convolution of the beam pattern with the terrain features. It produces data in polar coordinates containing beam blockage percentage for elevation angles spaced at 0.1 degrees up to an angle at which no blockage is evident.

As an example, Fig. 5 (below) shows the observed clutter power at each gate at a 0.4 degree elevation angle, for the NCAR S-POL radar at the FRONT site at Firestone in North-Eastern Colorado. (This is determined by running the clutter filter and computing the power removed by the filter.) By way of comparison, Fig. 6 shows the estimated beam blockage at each gate, for the same 0.4 degree elevation angle from the S-POL site. The clutter and computed beam blockage patterns in these two figures are highly similar, as expected.

Figure 7 shows the accumulated beam blockage along each radial, also at 0.4 degrees elevation. These are the blockage values that are used in the QPE algorithm.

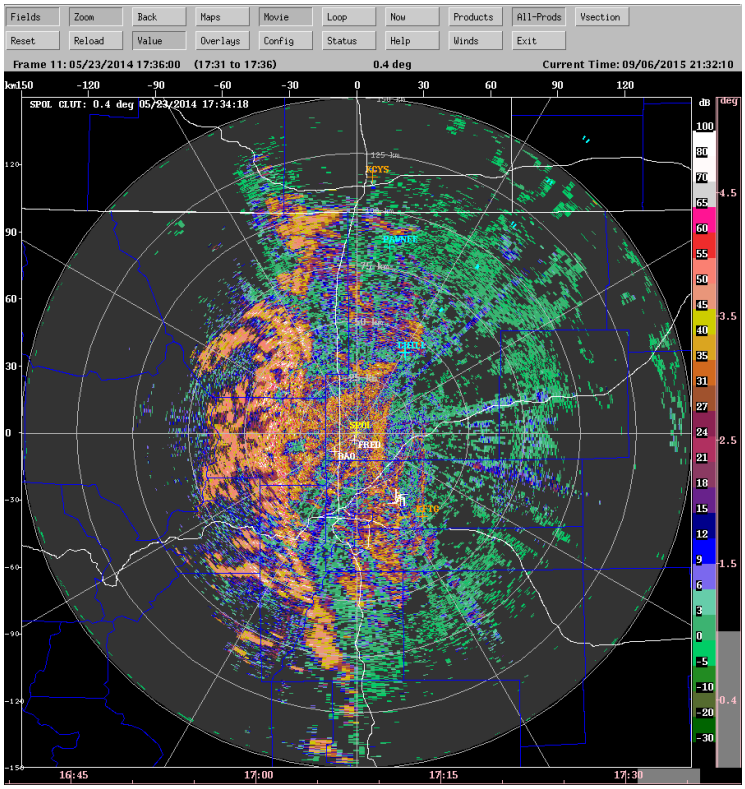

Figure 5: Observed clutter power – S-POL 0.4 deg. at the FRONT site at Firestone, Colorado.

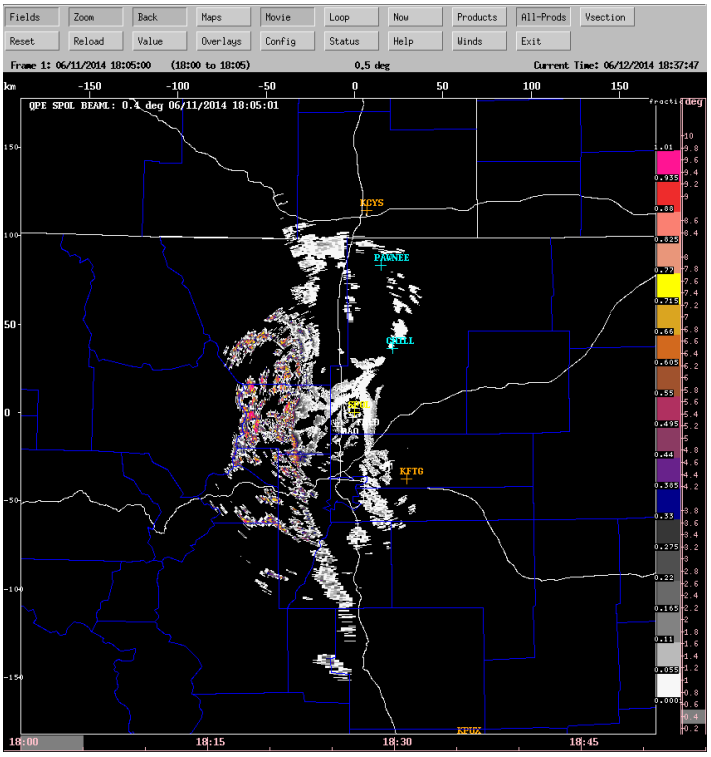

Figure 6: Computed beam blockage fraction at a gate – S-POL 0.4 deg.

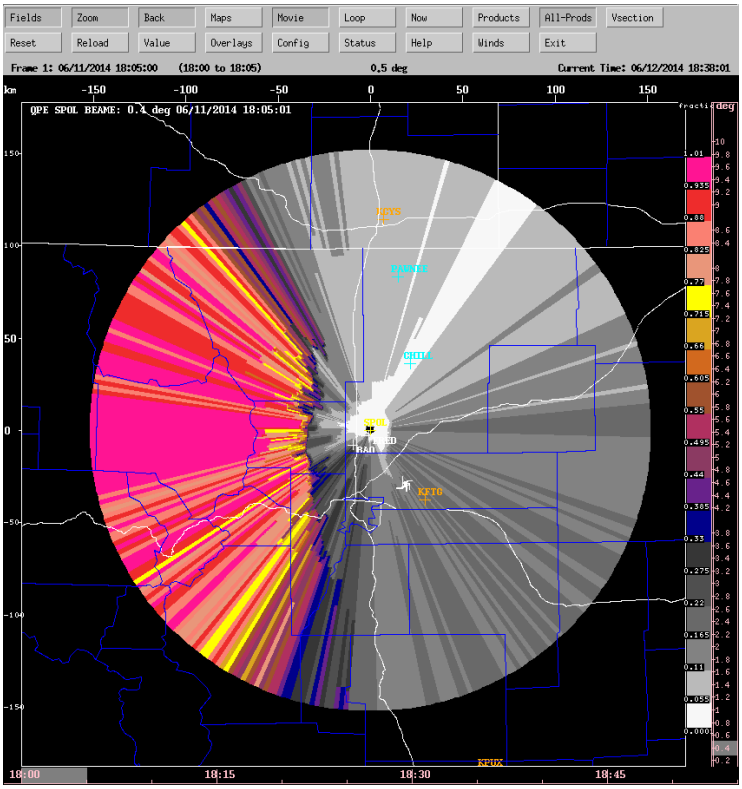

Figure 7: Accumulated blockage fraction for S-POL at 0.4 deg.

2.7 Computing the QPE at the surface

Figure 8 shows the decision logic for translating the QPE values from within the 3-D volume to the surface.

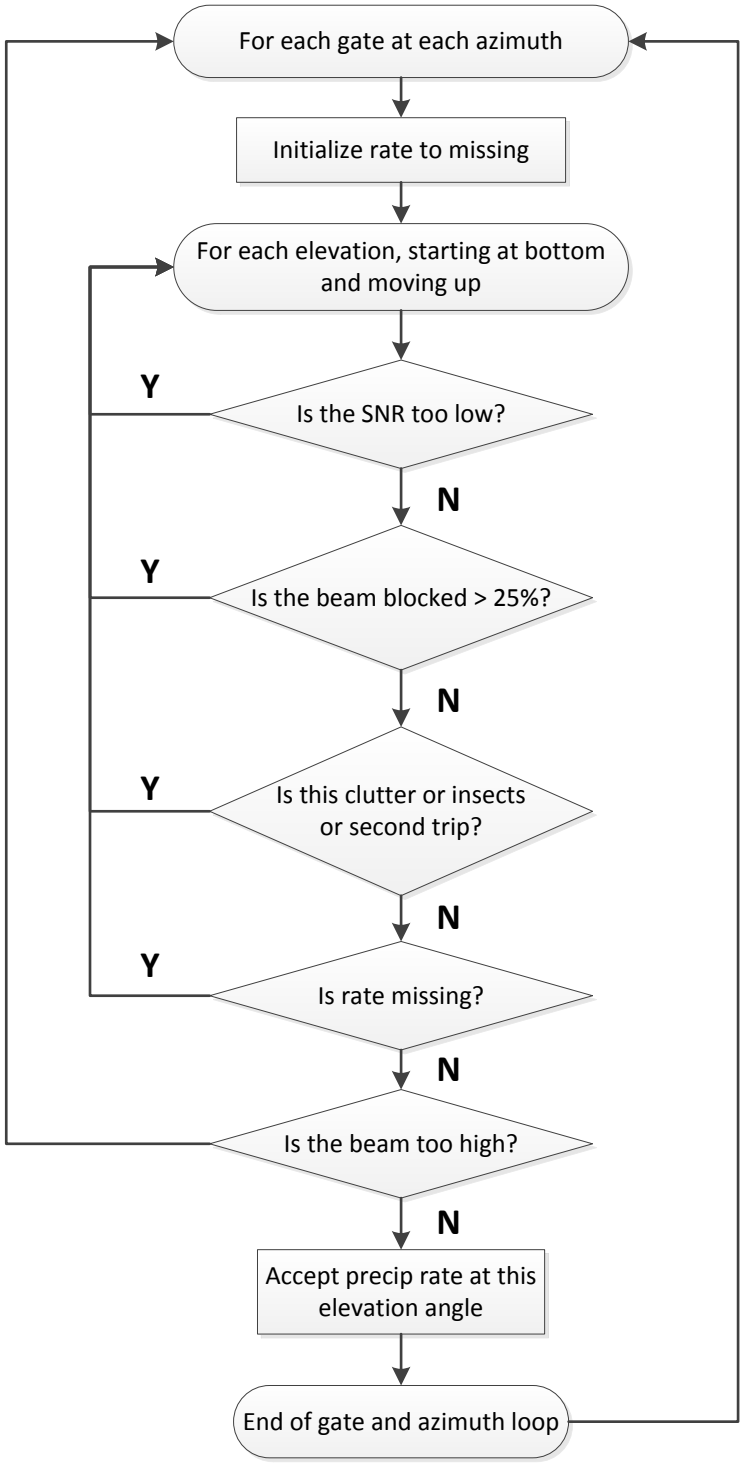

Figure 8: Decision logic for computing QPE at the surface.

The procedure is carried out for each range gate and each azimuth in the lowest PPI. Ideally the QPE from the lowest PPI is used as the surface estimate. However, this is not always possible for a variety of reasons. The following are checked:

- Is signal to noise ratio (SNR) < 5 dB ?
- Is beam blockage > 25% ?
- Does PID indicate clutter, insects or second trip?
- Is the QPE missing for this PPI?

If any of these conditions is true, the search moves up to the next PPI. If having moved up, the height of the gate exceeds a specified threshold (7 km) the QPE is set to missing.

In terms of beam blockage, if a gate has less than 25% blockage, it is treated as unblocked and accepted as a candidate for QPE. If the blockage exceeds 25%, the gate is regarded as unsuitable for QPE purposes. No attempt is made to adjust for beam blockage.

There is one important point to make about the logic for translating QPE to the surface. In the logic diagrams presented in sections 2.3 and 2.4, it can be seen that if hail is the predominant particle type and KDP is not available, the rate is set to a missing value. KDP sometimes cannot be calculated accurately because of clutter contamination at low elevation angles but is available at higher elevation angles. In this case, the algorithm will move to the next higher elevation angle in search of a valid precipitation rate. Since clutter contamination generally diminishes with increasing height, the KDP estimate may be better higher up than at the lowest elevation angle.

3 Results

3.1 Radar network for PECAN

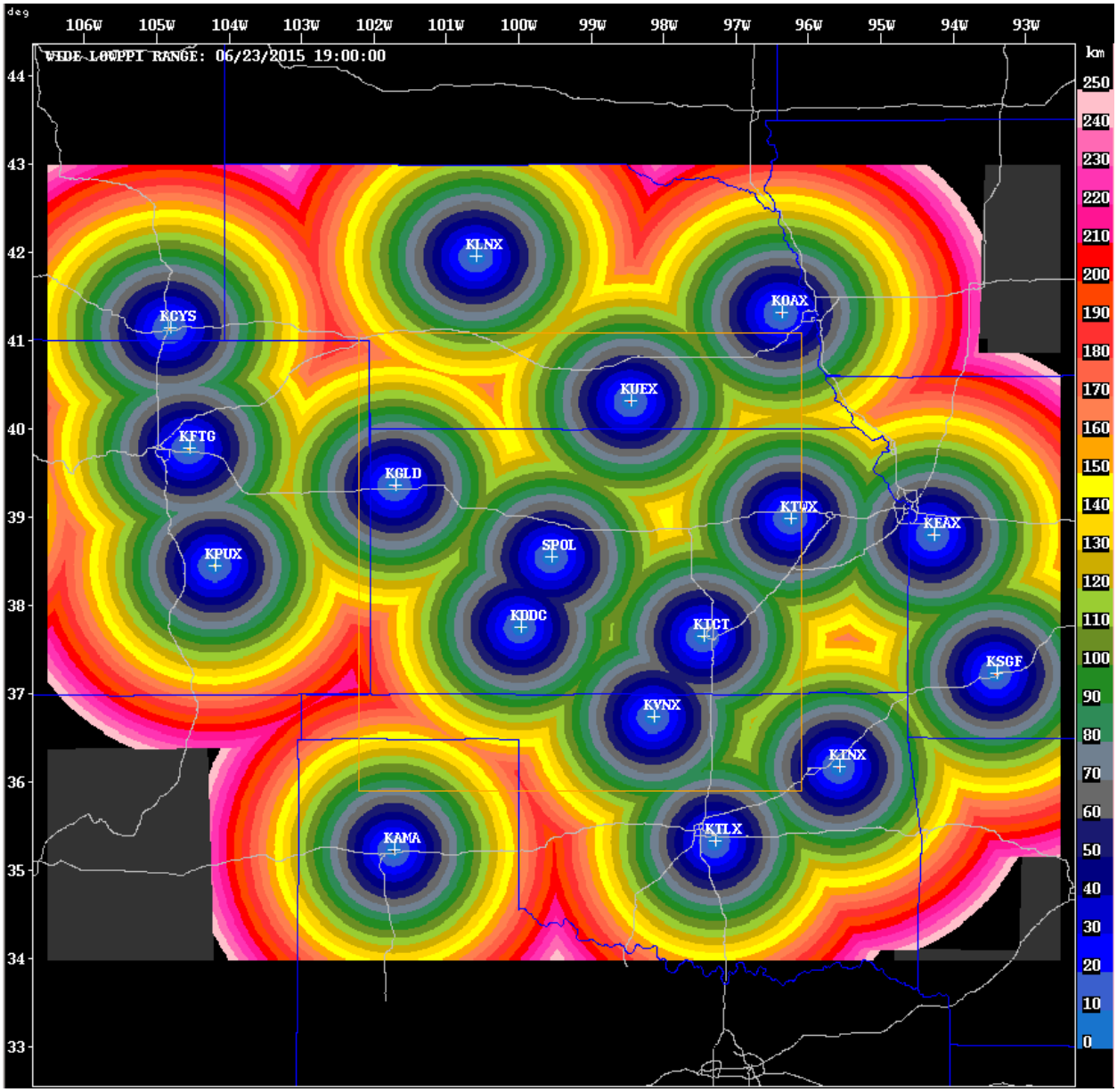

Figure 9: S-band radar network used for PECAN QPE product.

The QPE algorithm was run on the 17 S-band radars associated with the Plains Elevated Convection At Night (PECAN) field project, centered on Kansas.

Figure 9 shows the S-band radar network used for the QPE and other products for PECAN field project. The color scale shows the range from the closest radar.

Figure 10 shows an example of the large convective systems that occurred during PECAN. This is the column-maximum from the NOAA MRMS reflectivity mosaic, overlaid with lightning strikes (from the National Lightning Detection Network) from a 15-minute period.

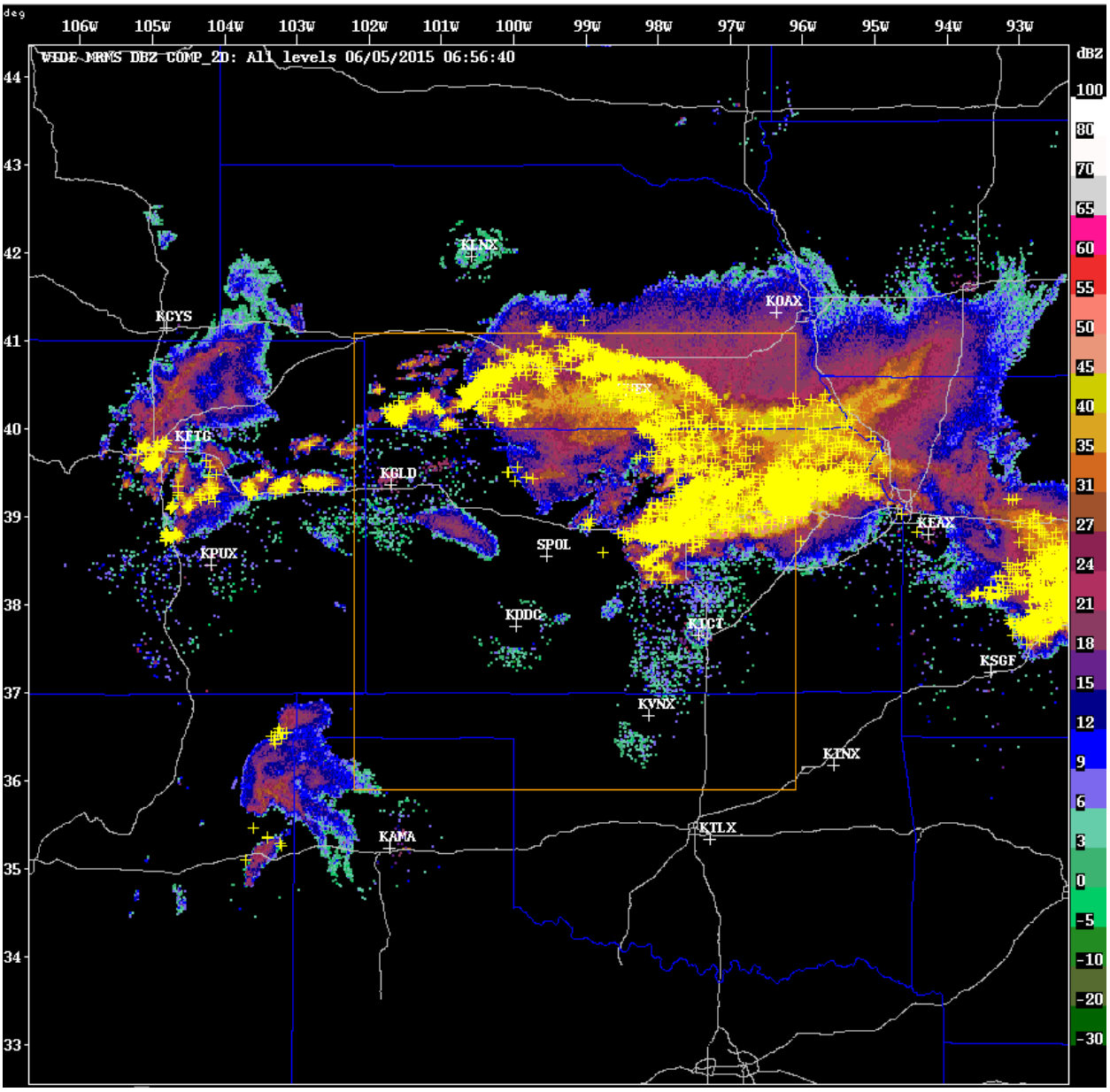

Figure 10: MRMS column-max reflectivity at 07:00 UTC on 2015/06/05.
NLDN lighting is overlaid as yellow crosses.

3.2 QPE products computed during PECAN

Figure 11 shows the 24-hour QPE accumulation from the NCAR HYBRID method at 00:00 UTC on 2015/06/06. This period includes the event shown above. The units are in mm.

The QPE products were produced for a number of accumulation periods: 1 hour, 2 hour, 3 hour and 24 hour running accumulations, and a 24-hour daily accumulation that restarts from zero at

00:00 UTC each day. The algorithms were run from mid-May to mid-July 2015, covering the 2-week period prior to the start of PECAN and the entire 6-week period of the main project.

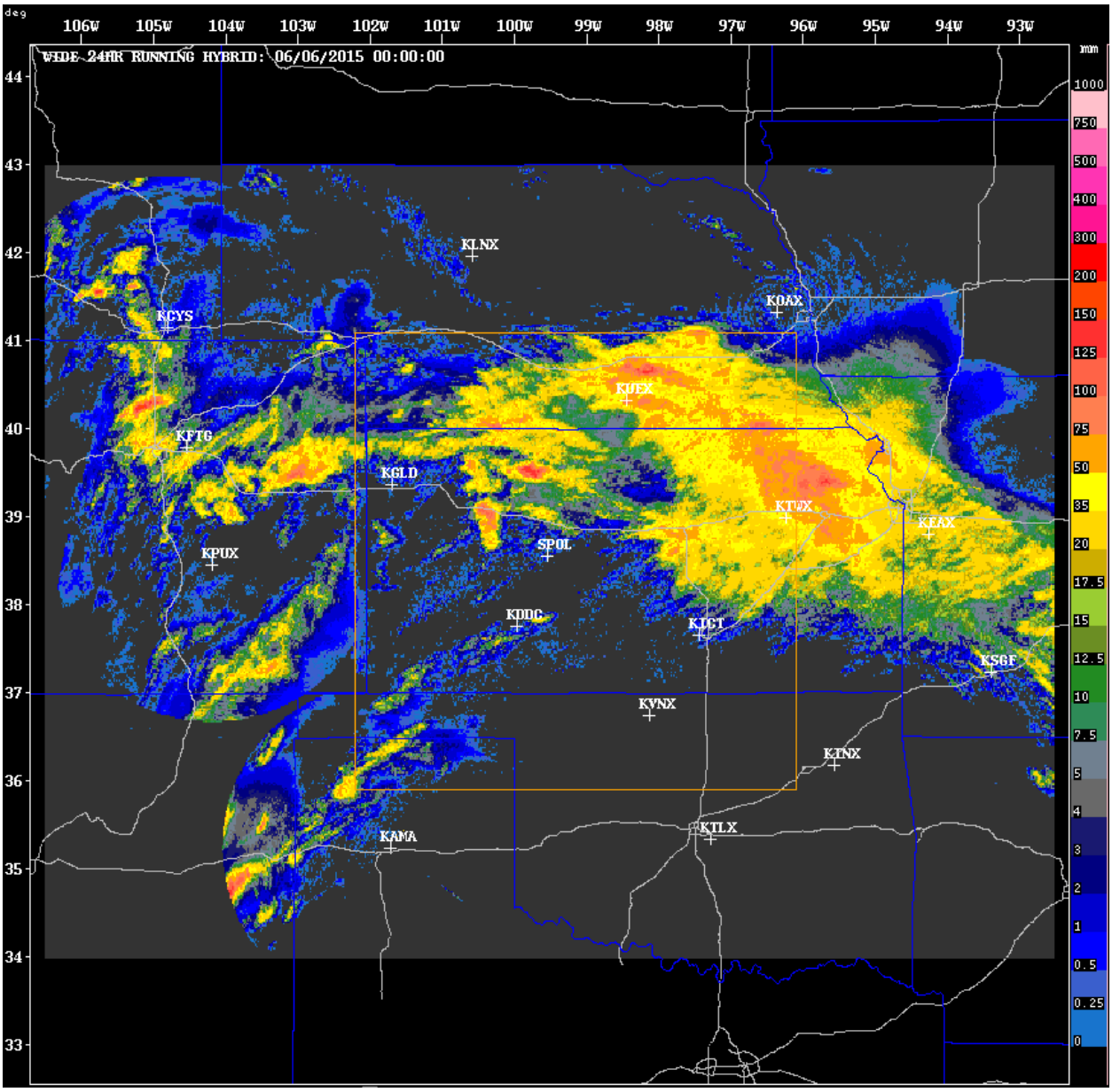

Figure 11: Accumulation (mm) from NCAR HYBRID QPE for the 24-hour period ending at 00:00 UTC on 2015/06/06.

3.3 Verification using surface precipitation gauges

Figure 12 shows the map of surface precipitation gauges available from NCDC for verification of the QPE product. Many of these sites only provide data on a 24-hour reporting cycle. Therefore it was decided to perform the verification on 24-hour QPE accumulations only.

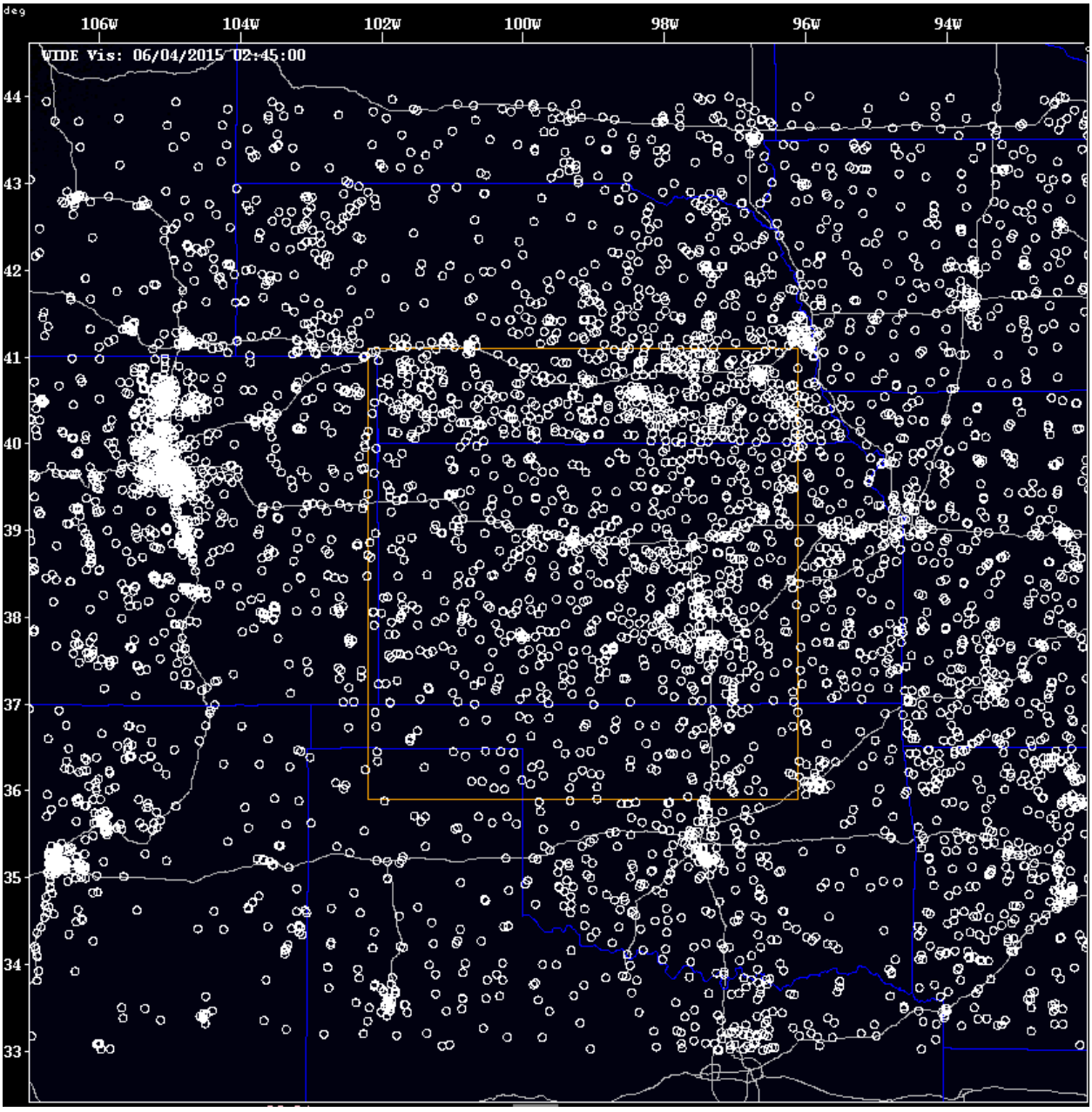

Figure 12: Map of daily precipitation gauge sites for the QPE domain. Data for these sites is available from NCDC.

The reporting times for these gauges are frequently in local standard time, so the times must be corrected to UTC before use in the verification process.

For the purposes of this paper, it was decided to perform the verification over the PECAN primary domain (see orange rectangle). The reasons for this are (a) there is good overlapping radar coverage for this domain and (b) the terrain in this region is reasonably flat, therefore the complications associated with the mountainous terrain of the Colorado Front Range are avoided.

Figure 13 shows the 24-hour gauge-reported values for the PECAN primary study domain, overlaid on the 24-hour accumulated QPE for 12:00 UTC (07:00 local time). Many of the manually-read gauges are reported around 07:00 local.

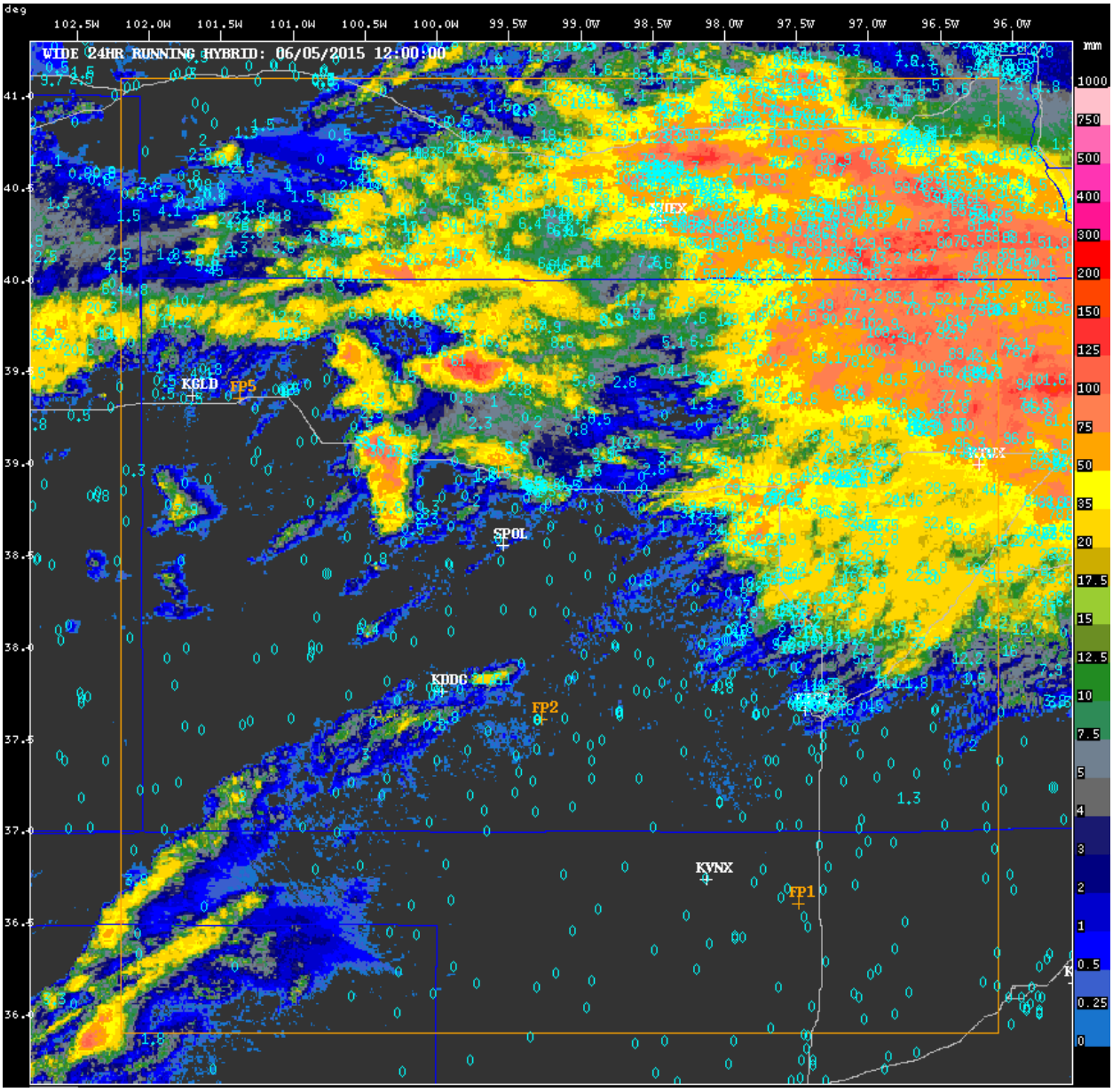

Figure 13: Measured gauge precipitation amounts overlaid on the radar-derived QPE map, for 12:00 UTC (07:00 local) on 2015/06/05.

Figures 14 (a) through (d) show 2-Dimensional histograms of the 24-hour radar-based QPE vs. the recorded gauge values for 4 estimators: (a) the NCAR HYBRID algorithm, (b) the NCAR Weighted-PID algorithm, (c) R(Z) and (d) R(Z, ZDR).

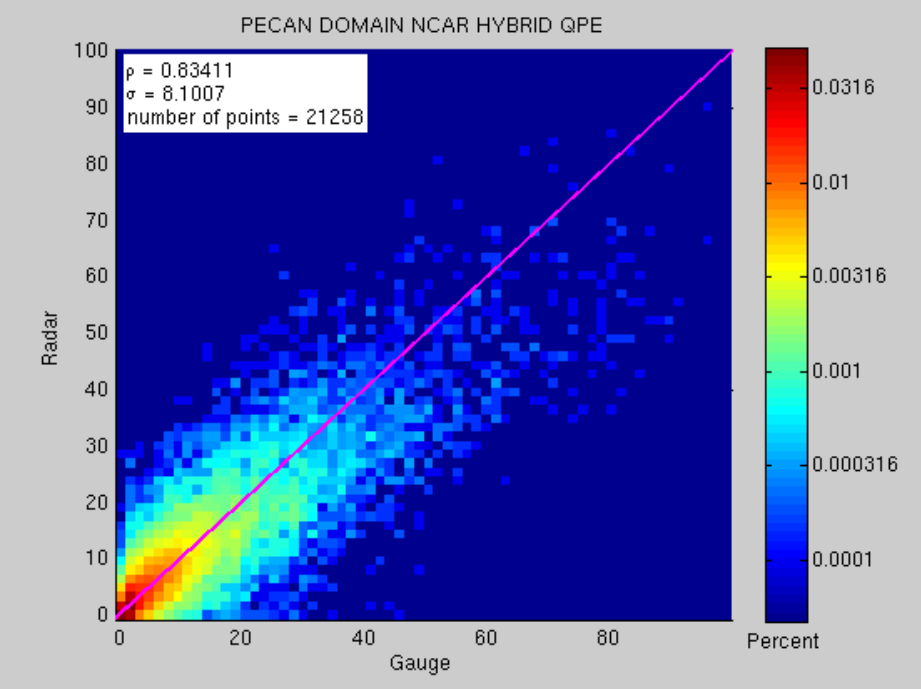

Figure 14(a): Radar-based 24-hour QPE vs gauge values, NCAR HYBRID algorithm.

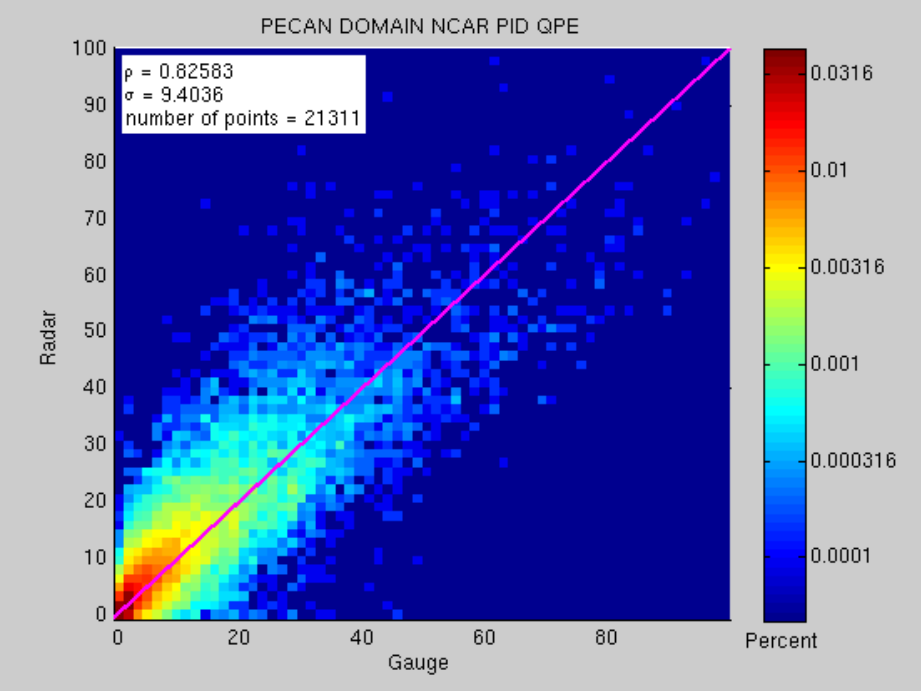

Figure 14(b): Radar-based 24-hour QPE vs gauge values, NCAR Weighted-PID algorithm.

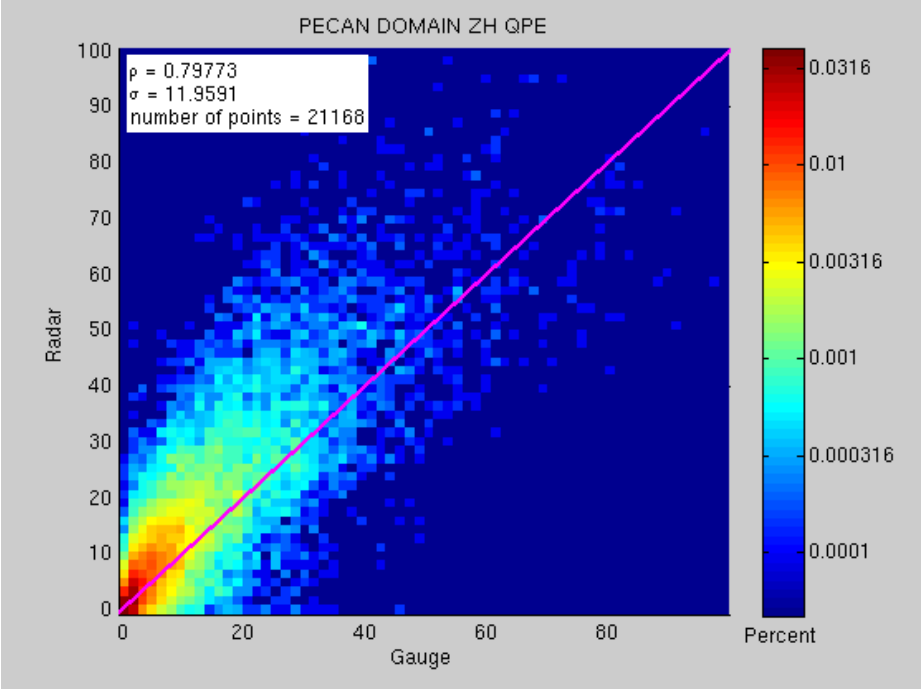

Figure 14(c): Radar-based 24-hour QPE vs gauge values, R(Z) estimator.

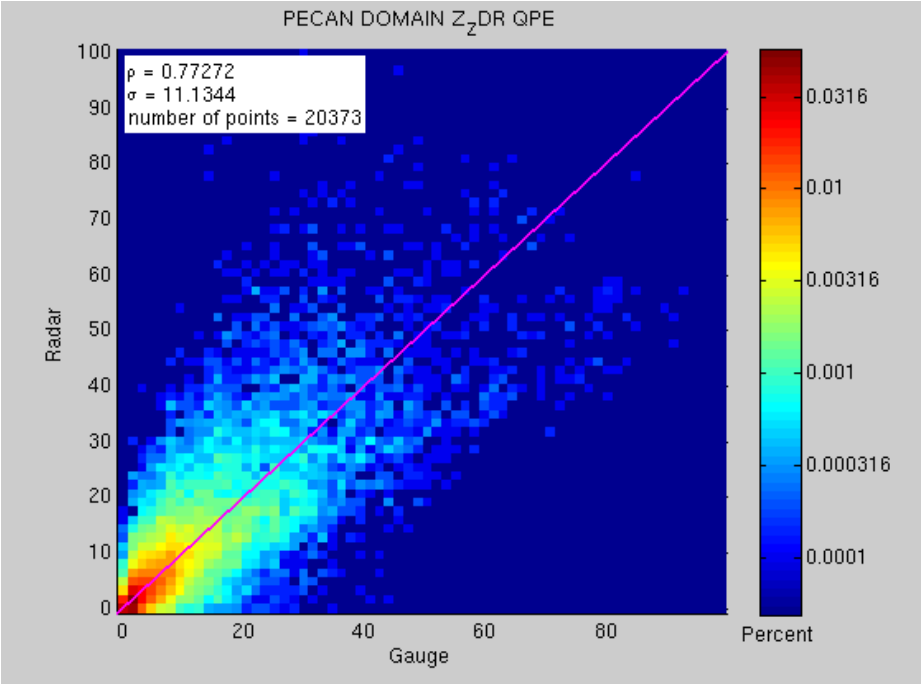

Figure 14(d): Radar-based 24-hour QPE vs gauge values, R(Z, ZDR) estimator.

Table 1 below summarizes the verification results for each of the four methods.

Method	N points	Correlation	Bias radar/gauge
NCAR HYBRID	21258	0.834	0.940
NCAR Weighted-PID	21311	0.826	1.108
R(Z)	21668	0.798	1.331
R(Z, ZDR)	21037	0.772	1.057

Table 1: Statistics for the various QPE methods.

Overall, the NCAR HYBRID algorithm performs the best, with good correlation statistics, and a bias that shows it under-estimates the gauge values by about 6 %. The Weighted-PID algorithm also has good correlation, but over-estimates the gauge measurements by about 11%. R(Z) on its own over-estimates by about 33%, as is generally expected, with poorer correlation than the PID-based methods. R(Z, ZDR) actually has a good bias value, with only a 6% over-estimate, but exhibits significantly poorer correlation, as can be seen by the larger spread in Figure 14(d).

Dealing with the melting layer is a challenge for precipitation estimation. Therefore, as an initial step in diagnosing why the estimators produce different results, it is instructive to consider their handling of widespread stratiform events, with the associated bright-band features. Fig. 15 shows such an event passing over KDDC on 2015/05/22. KDDC is at the center of the plot.

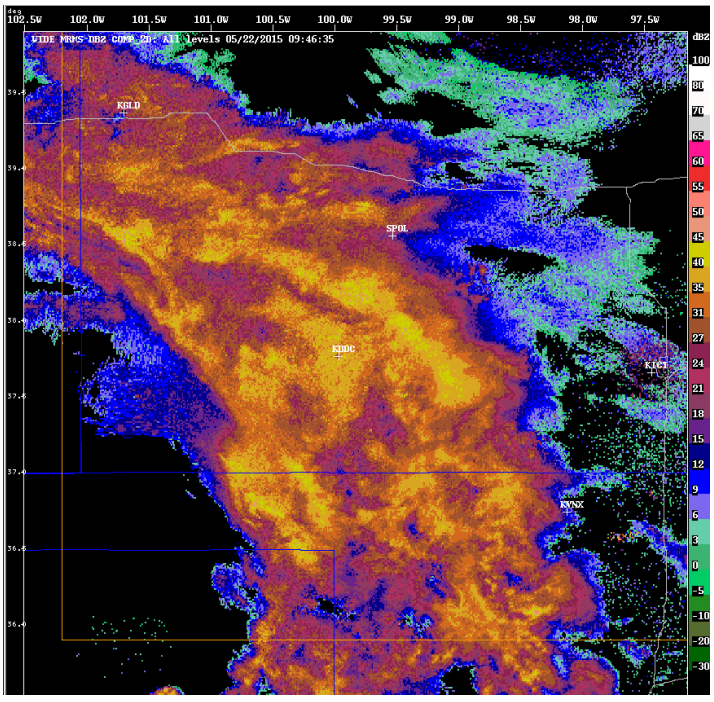

Figure 15: Large stratiform event passing over KDDC, the Dodge City NEXRAD 09:45 UTC on 2015/05/22.

Figures 16(a) through (d) below show the 24-hour QPE accumulation for this event, at 12:00 UTC on 2015/05/15, for the four estimators: (a) NCAR HYBRID, (b) NCAR Weighted-PID, (c) R(Z) and (d) R(Z, ZDR).

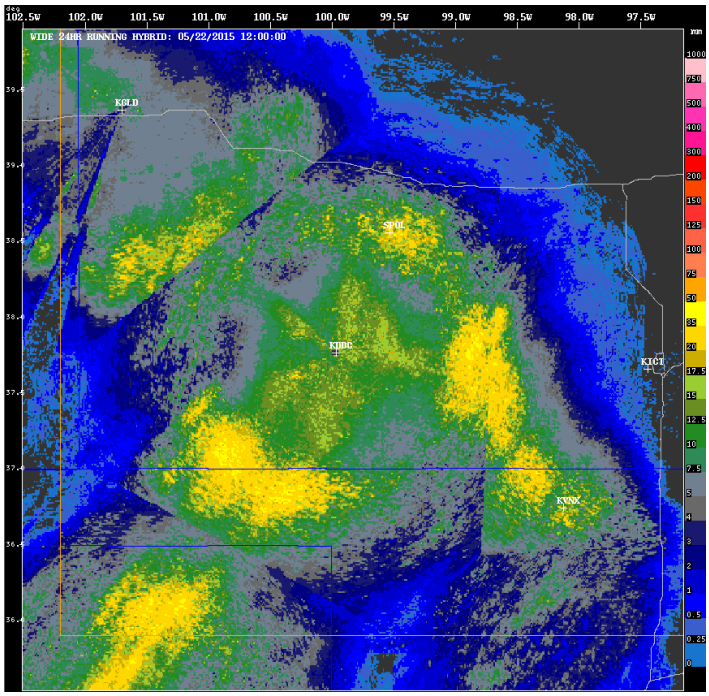

Figure 16(a): 24-hour QPE, NCAR HYBRID, for KDDC stratiform event, 2015/05/22.

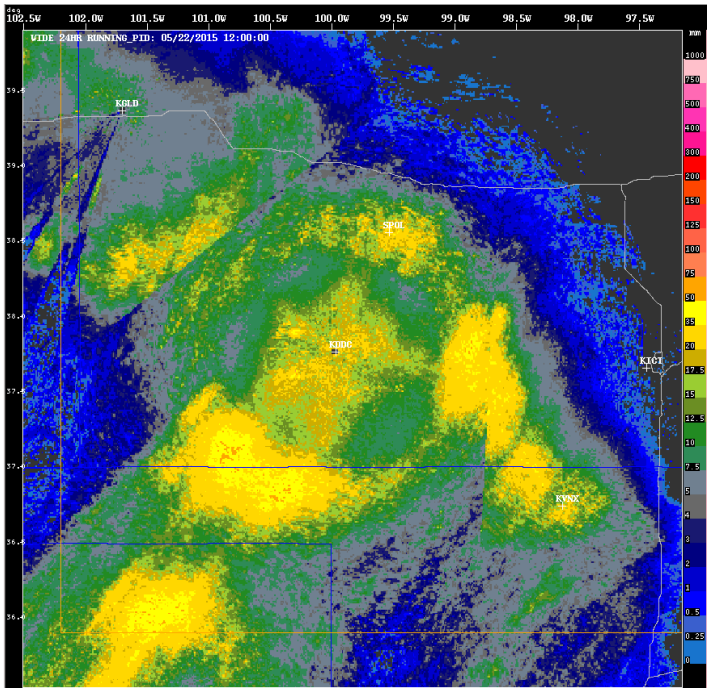

Figure 16(b): 24-hour QPE, NCAR Weighted-PID, for KDDC stratiform event, 2015/05/22.

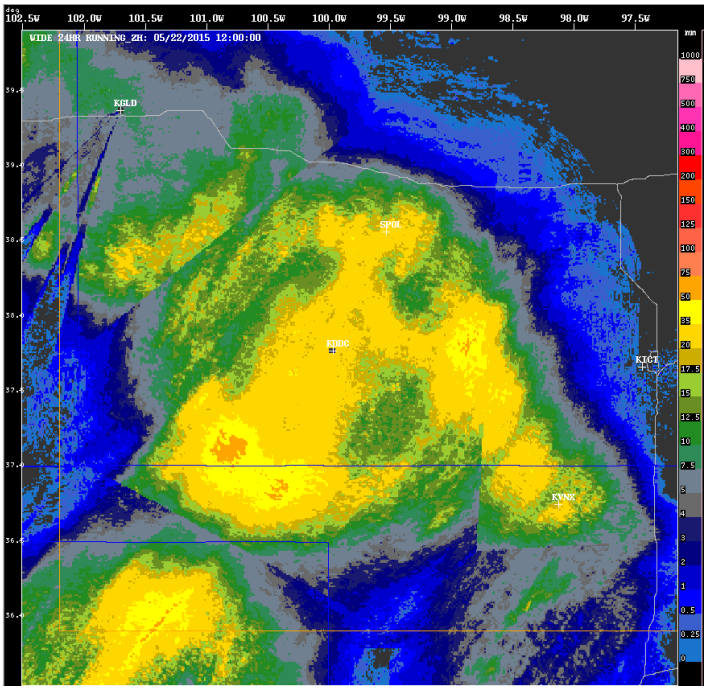

Figure 16(c): 24-hour QPE, R(Z), for KDDC stratiform event, 2015/05/22.

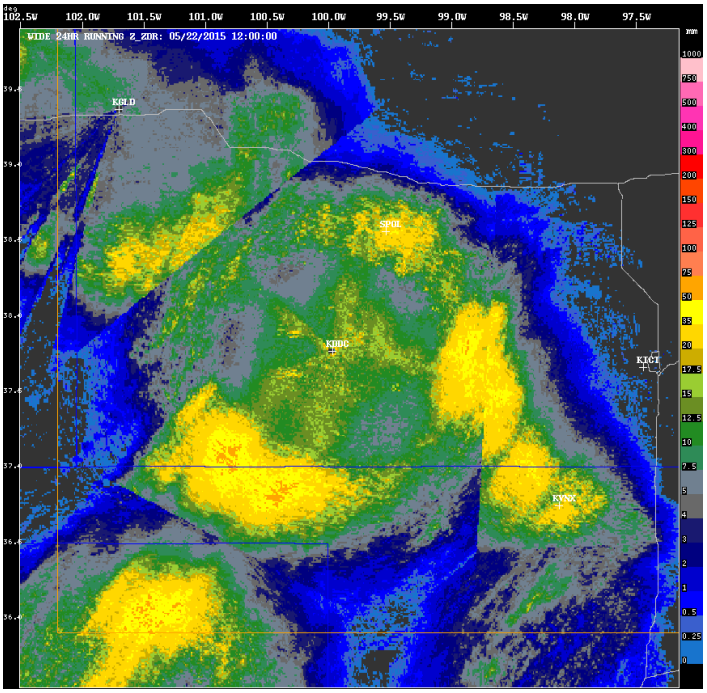

Figure 16(d): 24-hour QPE, R(Z, ZDR), for KDDC stratiform event, 2015/05/22.

Figures 16(a) through (d) demonstrate how clearly melting-layer effects can be seen in precipitation accumulation plots, even though these errors are not obvious in the QPE from individual radar volumes. This occurs because the range of the melting-layer ‘rings’ in CAPPIs

are similar from one volume to the next, so that the accumulation results in a definite feature. These features are useful in assessing QPE performance.

It can be seen that the HYBRID estimator handles the melting layer quite well, resulting in a reasonably muted 'ring' signature around the KDDC radar. The Weighted-PID estimator does not perform quite as well, and this would be one reason why this estimator has poorer validation statistics than the HYBRID. R(Z) performs quite poorly for this event, since there is no correction for the melting layer. R(Z, ZDR) performs somewhat better.

4 Conclusions

Building on the work of prior investigators and the National Weather Service NEXRAD program office, two QPE methods were developed. These rely on the NCAR Particle Identification (PID) algorithm to guide the selection of the radar-based estimators appropriate for precipitation estimation aloft in the radar volume. These algorithms were coupled with a technique for mapping the most appropriate values from their location aloft down to the surface.

These algorithms were run on the 17 radars associated with the PECAN field project, producing QPE products over the 2-month period from mid-May to mid-July 2015. These products were verified by comparison with 24-hour daily accumulation data for an extensive network of surface precipitation gauges. The results are promising, showing good correlation between the radar-based QPE and gauge measurements, and minor biases evident.

Future work will concentrate on further verification against surface measurements, and in making improvements to the algorithms to improve their performance. In addition this product will be compared for accuracy with the latest NOAA and MRMS products. It is likely that a single candidate will be chosen as the preferred method, and based on this study that is likely to be the NCAR HYBRID formulation.

5 Acknowledgements

Thank you to Kyoko Ikeda and Andrew Newman, both of the Research Applications Laboratory at NCAR, for their work to retrieve and reformat the gauge-measured precipitation data. Their work saved the authors considerable time and significantly improved this study.

NCAR is sponsored by the National Science Foundation.

6 References

Berkowitz, D. S., J. A Schultz, S. Vasiloff, K.L. Elmore, C.D. Payne and J.B. Boettcher, 2013: Status of Dual Pol QPE in the WSR-88D Network. *AMS 27th conference on hydrology, Austin, Texas*, 2.2.

Brandes, E. A., G.Zhang, J. Vivekanandan, 2002: Experiments in rainfall estimation with a polarimetric radar in a subtropical environment, *J. Appl. Meteor*., 41,674-685.

Bringi, V. N., C. R. Williams, M. Thurai, P. T. May, 2009: Using Dual-Polarized Radar and Dual-Frequency Profiler for DSD Characterization: A Case Study from Darwin, Australia. *J. Atmos. Technol*, Vol 26, No 10, October, 2107–2122.

Chandrasekar, V., E. Gorgucci, G. Scarchilli, 1993: Optimization of multi-parameter radar estimates of rainfall. *J. Appl. Meteor*., 32, 1288-1293.

Cifelli, R., V. Chandrasekar, S. Lim, P. C. Kennedy, Y. Wang, S. A. Rutledge, 2011: A New Dual-Polarization Radar Rainfall Algorithm: Application in Colorado Precipitation Events. *J. Atmos. Technol*, Vol 28, No 3, March, 352-364.

Giangrande S. E. and A. V. Ryzhkov, 2008: Estimation of rainfall based on the results of polarimetric echo classification. *J. Appl. Meteor. Climatol.,*, 47, 2445 – 2462.

Hubbert, J., V. Chandrasekar and V. N. Bringi, 1993: Processing and Interpretation of Coherent Dual-Polarized Radar Measurements. *J. Atmos. Technol*, Vol 10, No 2, April, 156-164.

Hubbert, J. C., P. Kennedy, M. Dixon, W.-C. Lee, S. Rutledge, T. Weckwerth, V. Chandrasekar and V. Loew, 2014. *P09, 8th European Conference on Radar in Meteorology and Hydrology*, Garmisch-Partenkirchen, Germany.

Kim D. and M. Maki, 2012: Validation of composite polarimetric parameters and rainfall rates from an X-band dual-polarization radar network in the Tokyo metropolitan area. *Hydrological Research Letters*, 6, 76-81.

Lim, S., V. Chandrasekar, and V. N. Bringi, 2005: Hydrometeor classification system using dual-polarization measurements: Model improvements and in-situ verification. *IEEE Trans. Geosci. Remote Sens*., 43, 792 – 801.

Park H., A. V. Ryzhkov, D. S. Zrnic and K Kim, 2009: The hydrometeor classification algorithm for the polarimetric WSR-88D: description and application to an MCS. *Weather and forecasting*, 24, 730 – 748.

Pepler, A. S., P. T. May, M. Thurai, 2011: A robust error-based rain estimation method for polarimetric radar. Part I: Development of a method. *J. Appl. Meteor. Climatol.*, 50, 2092-2103

Ryzhkov, A. V., T. J. Schuur, D. W. Burgess, P. L. Heinselman, S. E. Giangrande and D. S. Zrnic, 2005: The joint polarization experiment: Polarimetric rainfall measurement and hydrometeor classification. *Bull. Amer. Meteor. Soc.*, 86, 809 – 824.

Ryzhkov, A. V., D. S. Zrnic, 1995: Comparison of dual-polarization estimators of rain. *J. Atmos. Oceanic Technol*., 12, 249-256.

Sachidananda, M., D.S. Zrnic, 1987: Rain rate estimates from differential polarization measurements. *J. Atmos. Oceanic Technol*., 4, 588-598.

Vivekanandan, J., D. S. Zrnic, S. M. Ellis, R. Oye, A. V. Ryzhkov and J. Straka, 1999: Cloud microphysics retrieval using S-band dual-polarization radar measurements. *Bull. Amer. Meteor. Soc.*, 80, 381 – 388.